Thermal Behavior and Molecular Interaction of Poly(3-hydroxybutyrate- c o -3-hydroxyhexanoate) Studied by Wide-Angle X-ray Diffraction

ARTICLE *in* MACROMOLECULES · APRIL 2004

Impact Factor: 5.8 · DOI: 10.1021/ma049863t

8 AUTHORS, INCLUDING:

Adchara Padermshoke
Hiroshima University
11 PUBLICATIONS **357** CITATIONS
SEE PROFILE

Sanong Ekgasit
Chulalongkorn University
87 PUBLICATIONS **1,139** CITATIONS
SEE PROFILE

Isao Noda
University of Delaware
350 PUBLICATIONS **9,249** CITATIONS
SEE PROFILE

Yukihiro Ozaki
Kwansei Gakuin University
919 PUBLICATIONS **17,823** CITATIONS
SEE PROFILE

Thermal Behavior and Molecular Interaction of Poly(3-hydroxybutyrate-*co*-3-hydroxyhexanoate) Studied by Wide-Angle X-ray Diffraction

Harumi Sato,[†] Masayuki Nakamura,[‡] Adchara Padermshoke,[†,§] Hiroshi Yamaguchi,[†] Hikaru Terauchi,[‡] Sanong Ekgasit,[§] Isao Noda,[⊥] and Yukihiro Ozaki*[,†]

Department of Chemistry, School of Science and Technology, Kwansei-Gakuin University, Sanda, Hyogo 669-1337, Japan; Department of Physics, School of Science and Technology, Kwansei-Gakuin University, Sanda, Hyogo 669-1337, Japan; Sensor Research Unit, Department of Chemistry, Faculty of Science, Chulalongkorn University, Patumwan, Bangkok 10330, Thailand; and The Procter and Gamble Company, 8611 Beckett Road, West Chester, Ohio 45069

Received January 19, 2004; Revised Manuscript Received March 5, 2004

ABSTRACT: The thermal behavior and molecular interaction of a new type of bacterial copolyester, poly(3-hydroxybutyrate-*co*-3-hydroxyhexanoate), P(HB-*co*-HHx) (HHx = 12 mol %), was investigated by using wide-angle X-ray diffraction (WAXD) and differential scanning calorimetry (DSC). The WAXD measurements were carried out over a temperature range from 25 to 110 °C in the scattering angle range of $2\theta = 5-13°$. The WAXD pattern at room temperature shows that the P(HB-*co*-HHx) copolymer has an orthorhombic system ($\alpha = \beta = \gamma = 90°$) with $a = 5.76$ Å, $b = 13.20$ Å, and $c = 5.96$ Å (fiber repeat), which is identical to the crystal system of poly(3-hydroxybutyrate) (PHB) homopolymer. However, temperature-dependent variations in the lattice parameters, *a* and *b*, of P(HB-*co*-HHx) are quite different from those of PHB. Only the *a* lattice parameter increases with temperature, while the *b* lattice parameter changes very little in the case of crystalline P(HB-*co*-HHx). It seems that the intermolecular and intramolecular interactions between the C═O group and the CH_3 group decrease along the *a* axis of crystalline P(HB-*co*-HHx) with temperature. The (110) peak area of P(HB-*co*-HHx) starts decreasing from around 50 °C while that of PHB changes little at least until 140 °C, indicating that the crystallinity of PHB remains almost unchanged until 140 °C, but that of P(HB-*co*-HHx) decreases gradually from fairly low temperature (∼50 °C). The DSC measurement of the chloroform solution cast P(HB-*co*-HHx) shows a recrystallization peak around 51 °C. The (110) peak area of WAXD pattern of the chloroform solution cast P(HB-*co*-HHx) shows a maximum value at around 54 °C. The maximum of the (110) peak area demonstrates the recrystallization process of P(HB-*co*-HHx). The result is in a good agreement with the result of the DSC measurement.

Introduction

Poly(3-hydroxybutyrate) (PHB) and its copolymers, poly(hydroxyalkanoate)s (PHA)s, are biologically synthesized polyesters produced by a number of microorganisms and are consequently subjected to degradation by bacteria in the soil.[1−5] PHAs are completely biodegradable under aerobic and anaerobic conditions and can be produced from renewable resources. Among all natural polymers, only PHA polymers possess thermoplasticity and mechanical properties similar to those of synthetic polymers.[6−8] Since these polymers are biodegradable, they have been receiving much attention as new environmentally friendly materials, and numerous industrial applications, including new medical applications, are explored.[9]

PHB is one of the most well-studied bacterial polyesters in the PHA polymer. The thermal properties of PHB have been investigated by several research groups.[8,10−12] It has been claimed that PHB has similar thermal and mechanical properties to isotactic polypropylene (iPP).[13] The crystal structure of PHB was investigated by X-ray diffraction, and it was found that PHB has an orthorhombic system, $P2_12_12_1(D_2^4)$ with a fiber repeat of 5.96 Å.[14,15] PHB shows high crystallinity because of the perfect stereoregularity produced by bacteria. The high crystallinity of PHB makes it rigid and stiff, not necessarily well-suited for certain applications as a commodity plastic. To reduce the excess crystallinity and modify the overall physical properties of PHB,[13] other monomers are sometimes copolymerized with PHB. The PHB-based copolymers show a wide range of physical properties depending on the chemical structure of the comonomer units as well as the comonomer composition.[16] The copolymerization of 3-hydroxyvalerate (3HV) units in the molecular chain of PHB was introduced to regulate the physical properties of PHB, especially the excess crystallinity and T_m.[17] Unfortunately, the desired effect of 3HV incorporation was surprisingly limited due to the crystalline isodimorphism of 3HB and 3HV units.[18]

Recently, the Procter and Gamble Co. (Cincinnati, OH) has introduced a new kind of PHA copolymer with a small amount of medium length side groups, which has been commercialized under the trade name Nodax.[19] This class of copolymers demonstrate some attractive properties, for example, anaerobic and aerobic degradability, alkaline digestability, hydrolytic stability, good odor and oxygen barrier, ideal surface properties for printability, and so on. It further shows substantially

[†] Department of Chemistry, Kwansei-Gakuin University.
[‡] Department of Physics, Kwansei-Gakuin University.
[§] Chulalongkorn University.
[⊥] The Procter and Gamble Company.
* To whom correspondence should be addressed: FAX +81-79-565-9077, e-mail ozaki@ksc.kwansei.ac.jp.

10.1021/ma049863t CCC: $27.50
Published on Web 04/22/2004

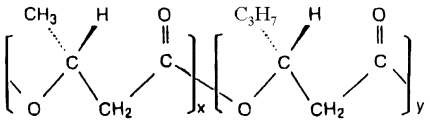

Figure 1. Molecular structure of poly(3-hydroxybutyrate-*co*-3-hydroxyhexanoate), P(HB-*co*-HHx) (HHx = 12 mol %).

reduced crystallinity and increased flexibility compared to the PHB homopolymer. Furthermore, Nodax has excellent compatibility with other biodegradable polymers and synthetic polymers.[19] Nodax may be used in a variety of polymer applications because they can control their mechanical properties by changing the comonomer composition and can be processed into fibers and films as well as molded plastic products. These new products are expected to be used not only for biodegradable polymers but also for medical materials in terms of their biocompatibility.

One of the representative members of the Nodax copolymer family is the poly(3-hydroxybutyrate-*co*-3-hydroxyhexanoate) or P(HB-*co*-HHx), which is a random copolymer of [*R*]-3-hydroxybutyrate and [*R*]-3-hydroxyhexanoate units. Figure 1 shows a molecular structure of P(HB-*co*-HHx) (HHx = 12 mol %). The biodegradation mechanism, chemical synthesis, and mechanical properties of P(HB-*co*-HHx) were reported by several research groups.[20−22] The thermal behavior of P(HB-*co*-HHx) was also investigated by differential scanning calorimetry (DSC).[20,22] However, so far there is no literature describing X-ray diffraction studies and infrared (IR) studies of the thermal behavior of P(HB-*co*-HHx). The WAXD measurements of PHA polymers were carried out only at room temperature to characterize their crystallinity and crystal structure.[23]

Investigations of temperature-dependent variations in the X-ray diffraction pattern and IR spectrum are very important to explore the crystal-to-amorphous transition and variations in the inter- and intramolecular interactions. The unit cell dimensions change with temperature as a result of thermal expansion, and the thermal expansion of the polymer is often highly anisotropic. We have investigated the thermal properties of one of the new types of bacterial copolyesters, P(HB-*co*-HHx) (HHx = 12 mol %), by using wide-angle X-ray diffraction (WAXD), DSC, and IR spectroscopy. The present study reveals unique constraint factors of the atoms and molecules observed in the crystal structure of P(HB-*co*-HHx). The IR study will be reported separately.[24]

Experimental Section

Samples. Bacterially synthesized P(HB-*co*-HHx) and PHB were obtained from the Procter and Gamble Co. The P(HB-*co*-HHx) sample was dissolved in hot chloroform, reprecipitated in methanol as fine powder, and vacuum-dried at 60 °C. The purified P(HB-*co*-HHx) and PHB samples thus obtained were used for all the experiments. Some of the purified powder sample was redissolved in chloroform and then cast as a film by evaporating the solvent.

Wide-Angle X-ray Diffraction (WAXD). A WAXD pattern and an X-ray diffraction trace of the precipitated powder of P(HB-*co*-HHx) were measured at room temperature in the scattering angle range of $2\theta = 5-35°$ by using a Rigaku R-Axis IV imaging plate diffractometer. Cu Kα radiation (wavelength 1.5418 Å) from a Rigaku Ultra-X18 rotating anode X-ray generator was used as an incident X-ray source (40 kV, 100 mA) (Figure 2a,b). The temperature-dependent WAXD data were measured for the precipitated powder samples of P(HB-*co*-HHx) over a temperature range from 25.0 to 110.0 °C in the scattering angle range of $2\theta = 5-13°$ by using a two-circle Rigaku X-ray diffractometer equipped with a scintillation detector (RINT2000/PC). For comparison, the corresponding WAXD data were collected for the precipitated powder sample of PHB over a temperature range from 28.3 to 174.3 °C in the scattering angle range of $2\theta = 2-13°$ by using the two-circle Rigaku X-ray diffractometer. Mo Kα radiation (wavelength 0.710 69 Å) was used as an incident X-ray source (40 kV, 240 mA). The X-ray diffraction patterns of chloroform solution cast P(HB-*co*-HHx) were obtained with the two-circle Rigaku X-ray diffractometer and an imaging plate over a temperature range of 30.1−105.8 °C in the range of $2\theta = 2-30°$. The silicone powder put in the samples was used for the calibration of the angle.

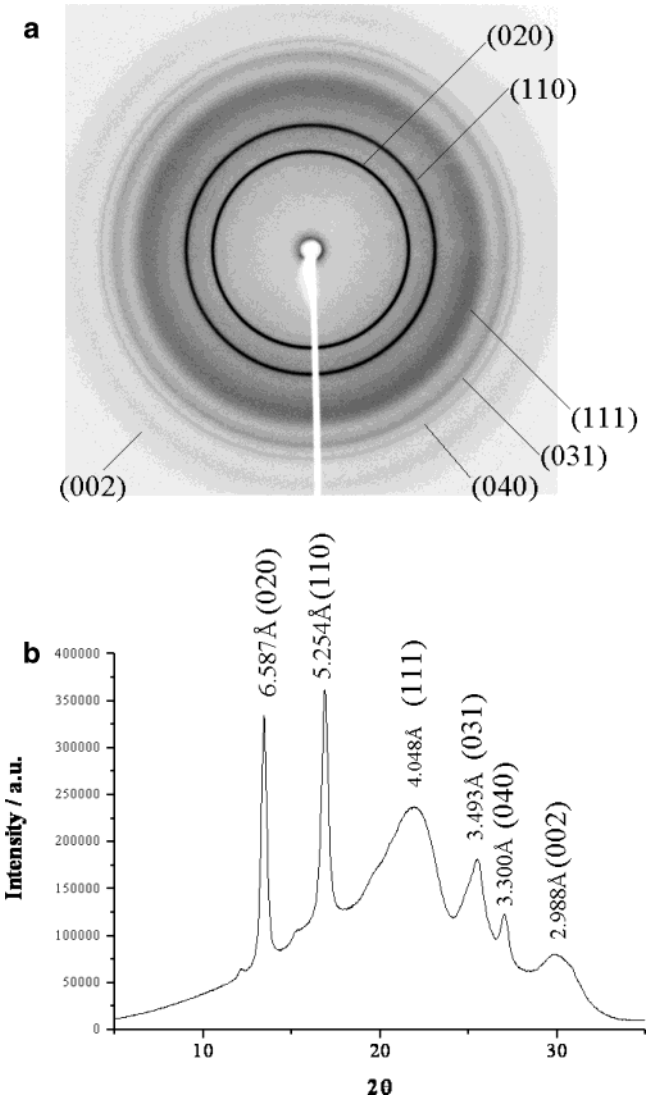

Figure 2. (a) An X-ray diffraction pattern of P(HB-*co*-HHx) (HHx = 12 mol %) powder sample at room temperature crystallized in the $P2_12_12_1$ orthorhombic system with the lattice parameters of $a = 5.76$ Å, $b = 13.20$ Å, $c = 5.96$ Å (fiber axis). (b) An X-ray diffraction trace of P(HB-*co*-HHx) (HHx = 12 mol %) powder sample at room temperature obtained by a radial microdensitometer scan of the powder diagram shown in (a).

The observed X-ray diffraction intensity $I(2\theta)$ was assumed to consist of $I_{peak}(2\theta)$ and $I_{BG}(2\theta)$

$$I(2\theta) = I_{peak}(2\theta) + I_{BG}(2\theta) \quad (1)$$

where $I_{peak}(2\theta)$ and $I_{BG}(2\theta)$ are the diffraction peak intensities due to the crystalline and amorphous parts of the sample, respectively. The contributions from the crystalline ($I_{peak}(2\theta)$)

and amorphous ($I_{BG}(2\theta)$) parts to the X-ray scattering were estimated by computer fitting using a Gaussian function shown in eq 2 and a quadratic function shown in eq 3, respectively:

$$I_{peak}(2\theta) = \frac{A}{\sigma\sqrt{\pi/2}} \exp\left[-2\left(\frac{2\theta - 2\theta_0}{\sigma}\right)^2\right] \quad (2)$$

where A, σ, and $2\theta_0$ are a peak area, a full-width at half-maximum of the reflection peak, and a center point of the peak, respectively. The background peak $I_{BG}(2\theta)$ is calculated by the following equation:

$$I_{BG}(2\theta) = a(T)(2\theta)^2 + b(T)(2\theta) + c(T) \quad (3)$$

where $a(T)$, $b(T)$, and $c(T)$ are scaling and correction factors for the baseline. The values A, σ, $2\theta_0$, $a(T)$, $b(T)$, and $c(T)$ were determined together by a nonlinear least-squares fit to eq 1.

Differential Scanning Calorimetry (DSC). Differential scanning calorimetry (DSC) measurements of P(HB-*co*-HHx) copolymer were performed with a Seiko EXDSTAR6000 apparatus with a DSC6200 module over a temperature range from −50 to 140 °C at heating and cooling rates of 10 and 20 °C min^{-1}, respectively. The samples used for the DSC measurements were the same as those for the WAXD analysis.

Results and Discussion

WAXD. Parts a and b of Figure 2 show respectively a WAXD pattern and an X-ray diffraction trace of P(HB-*co*-HHx) powder sample at room temperature. P(HB-*co*-HHx) powder sample shows a high level of crystallinity.[20,22] It was reported that the unit cells of PHB and poly(hydroxyvalerate) (PHV) belong to the orthorhombic system, $P2_12_12_1(D_2^4)$ ($\alpha = \beta = \gamma = 90°$), with $a = 5.76$ Å, $b = 13.20$ Å, $c = 5.96$ Å (fiber repeat) and $a = 9.52$ Å, $b = 10.08$ Å, $c = 5.56$ Å (fiber repeat).[14,15,25] The P(HB-*co*-HHx) (HHx = 12 mol %) also shows an orthorhombic system ($\alpha = \beta = \gamma = 90°$) with $a = 5.76$ Å, $b = 13.20$ Å, $c = 5.96$ Å (fiber repeat), which is the same as the PHB crystal system.[20] The P(HB-*co*-HV) copolymers with the HV composition from 0 to 37 mol % crystallize in the PHB lattice, while those with the HV composition from 53 to 95 mol % crystallize in the PHV lattice.[23] The (110) d spacing of P(HB-*co*-HV) copolymer apparently increases as the HV content increases to 37 mol %, while the (020) and (002) d spacings remain unchanged, indicating that only the parameters of the unit cell change.[18,23] As described above, P(HB-*co*-HHx) (HHx = 12 mol %) also shows only one crystalline form with the PHB lattice. It is reasonable to expect this result because the HHx content is 12 mol %. One may expect that the propyl side chains of HHx units expand the (110) d spacing of the PHB lattice in P(HB-*co*-HHx) even more so than that in P(HB-*co*-HV) due to the steric effects of the propyl side chains. However, as a matter of fact, the (110) d spacing of P(HB-*co*-HHx) is smaller than that of P(HB-*co*-HV).[23] It can be assumed that the propyl side chain of HHx has stronger inter- and intramolecular interactions than the ethyl side chain of HV, since the propyl side chain is located closer to the C═O group in the lattice constant a axis than the ethyl side chain. Another possibility is that the propyl side chains of HHx are protruded in the crystal structure, while the ethyl side chain of HV can be fixed in the crystal with PHB. Therefore, the (110) d spacing of P(HB-*co*-HHx) may show the proximity value with that of PHB.

Figure 3a shows a helical structure model of P(HB-*co*-HHx) copolymer proposed on the basis of the results of X-ray diffraction.[14,15,26,27] The WAXD pattern shows that the crystalline structure of P(HB-*co*-HHx) is orthorhombic, $P2_12_12_1(D_2^4)$, with $a = 5.76$ Å, $b = 13.20$ Å, $c = 5.96$ Å (fiber repeat).[20] Figure 3b shows a structure of PHB studied by Yokouchi et al.[14] Of note in Figure 3b is that the CH_3 group of PHB is close to the C═O group on the a axis.

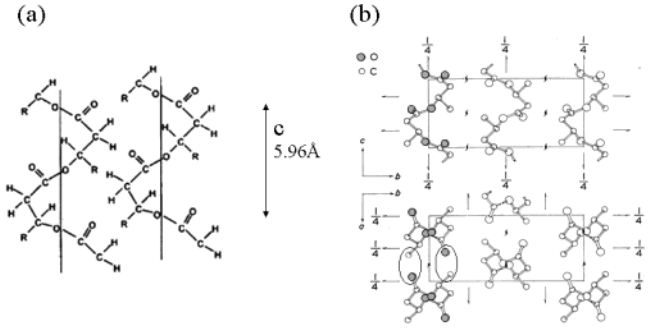

Figure 3. (a) Proposed helical structure model of P(HB-*co*-HHx) copolymer. (Reproduced from ref 27 with permission. Copyright 2001 John Wiley & Sons, Inc.) (b) Reported crystalline structure of PHB. The $P2_12_12_1$ orthorhombic system with the lattice parameters of $a = 5.76$ Å, $b = 13.20$ Å, $c = 5.96$ Å (fiber axis). (Reproduced from ref 14 with permission. Copyright 1973 Elsevier Science.)

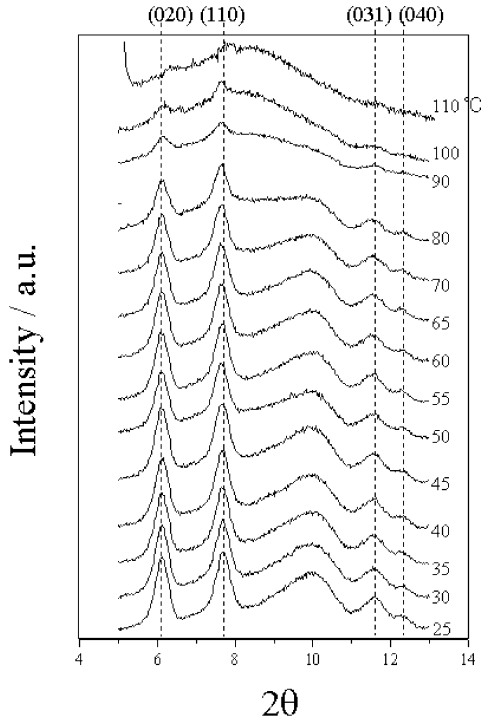

Figure 4. Temperature dependence of the X-ray diffraction of P(HB-*co*-HHx) powder sample measured over a temperature range from 25 to 110 °C.

Temperature-Dependent Variations in the WAXD of the Precipitated Sample. Figure 4 shows the temperature dependence of the WAXD pattern of the precipitated P(HB-*co*-HHx) sample. The WAXD patterns were measured over a temperature range from 25 to 110 °C in the scattering angle range of $2\theta = 5-13°$. It can be seen from Figure 4 that the (110) d spacing of P(HB-*co*-HHx) lattice expands as temperature increases. However, the (020), (040), and (031) d spacings of the sample do not change with temperature. The WAXD patterns in Figure 4 show that the peak due to the lattice constant a shifts to large value as temperature

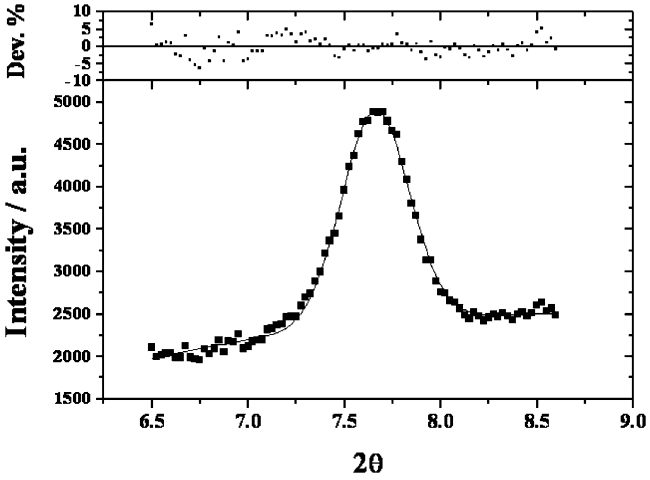

Figure 5. A representative (110) reflection of WAXD of P(HB-*co*-HHx) powder sample. The solid curve represents the one fitted by eq 1 with $A = 1102 \pm 22$, $\sigma = 0.350 \pm 0.005$, $2\theta_0 = 7.661 \pm 0.002$, $a(T) = -116.7 \pm 34.6$, $b(T) = 2013 \pm 524$, and $c(T) = -6178 \pm 1968$. Top panel: the relative errors of the fit.

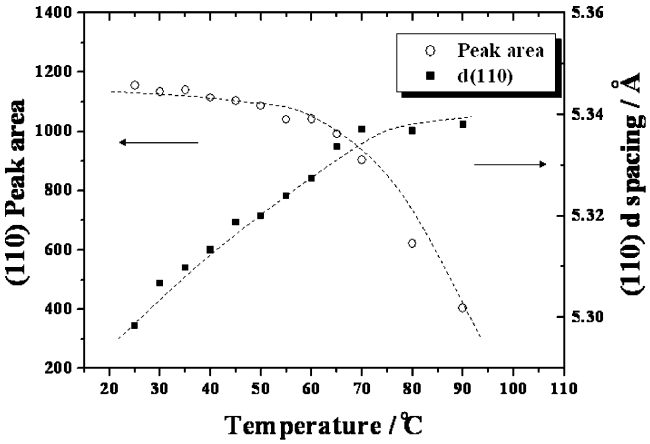

Figure 6. Temperature dependences of the peak area and *d* spacing of the (110) reflection of the P(HB-*co*-HHx) powder sample.

increases. In other words, only the lattice constant *a* of the unit cell changes with temperature in the P(HB-*co*-HHx) crystal. Referring to the crystalline structure of PHB (Figure 3),[14,15] one can assume that there are intermolecular and intramolecular interactions between the C═O group and the CH_3 group also in the P(HB-*co*-HHx) copolymer.

Figure 5 shows a representative (110) reflection peak and the result of its nonlinear least-squares fitting (see Experimental Section) of the P(HB-*co*-HHx) powder sample. The solid curve represents the one fitted by eq 1 with $A = 1102 \pm 22$, $\sigma = 0.350 \pm 0.005$, $2\theta_0 = 7.661 \pm 0.002$, $a(T) = -116.7 \pm 34.6$, $b(T) = 2013 \pm 524$, and $c(T) = -6178 \pm 1968$. The fitting is quite satisfactory as shown in the deviations in Figure 5.

Figure 6 shows variations in the (110) peak area and the (110) *d* spacing vs temperature for the precipitated sample. The peak area and peak maximum position respectively indicate the crystallinity and the thermal expansion of the sample. It is noted that the (110) *d* spacing expands gradually with temperature, while the peak area changes little until around 50 °C and shows a gradual decrease above about 50 °C.

Figure 7 shows the temperature dependences of the (020) peak area and the (020) *d* spacing for the precipitated sample. Note that the thermal behavior of the

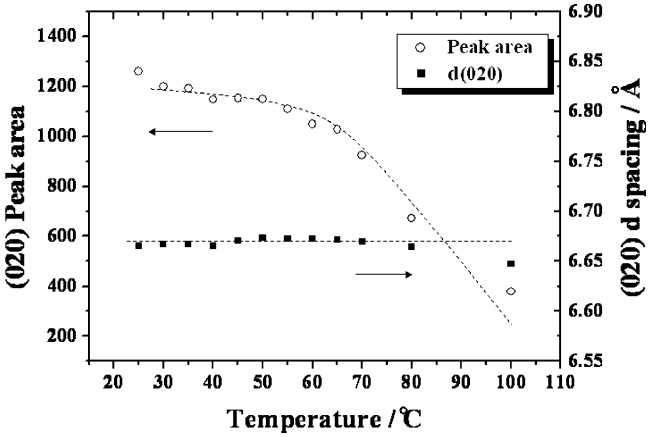

Figure 7. Temperature dependences of the peak area and *d* spacing of the (020) reflection of the P(HB-*co*-HHx) powder sample.

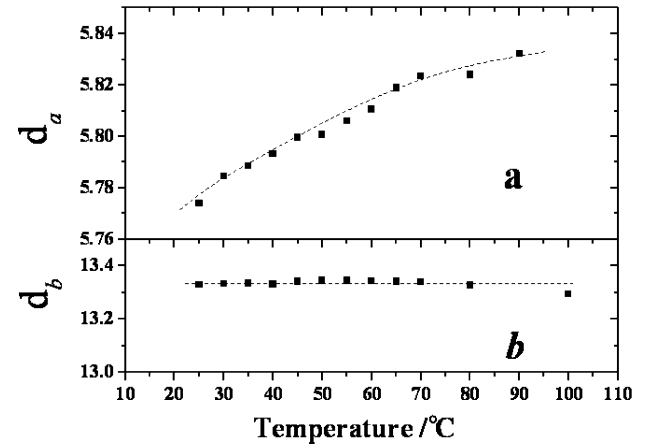

Figure 8. Changes in the lattice parameters, *a* and *b*, of the precipitated P(HB-*co*-HHx) sample vs temperature.

(020) peak area is similar to that of the (110) peak area. However, the (020) *d* spacing shows little thermal expansion compared to the (110) *d* spacing.

Figure 8 shows temperature-dependent variations in the lattice parameters, *a* and *b*, of the precipitated sample. It is clear from Figure 8 that the *a* lattice parameter increases gradually with the temperature increase while the *b* lattice parameter changes little. It is very likely that the increase in the *a* lattice parameter results from the decrease in the inter- and intramolecular interactions between the C═O group and the CH_3 group along the *a* axis of crystalline P(HB-*co*-HHx). The interaction is mainly concerned with the weak hydrogen bond between the C═O group and the CH_3 group, but there is the possibility that some C═O groups interact with the propyl group.

Temperature-Dependent Variations in WAXD of the Chloroform Solution Cast Film Sample. Figure 9 presents the temperature dependence of the (110) *d* spacing of the WAXD pattern of a P(HB-*co*-HHx) film cast from chloroform solution. Of note in Figure 9 is the thermal expansion of the (110) *d* spacing of P(HB-*co*-HHx). Variations in the (110) peak area and (110) *d* spacing vs temperature are shown in Figure 10 for the solution cast film sample. The temperature-dependent changes in the (110) peak area are quite different between the precipitated and solution cast samples (Figures 6 and 10). The peak area represents the crystallinity of the sample. The crystallinity of the

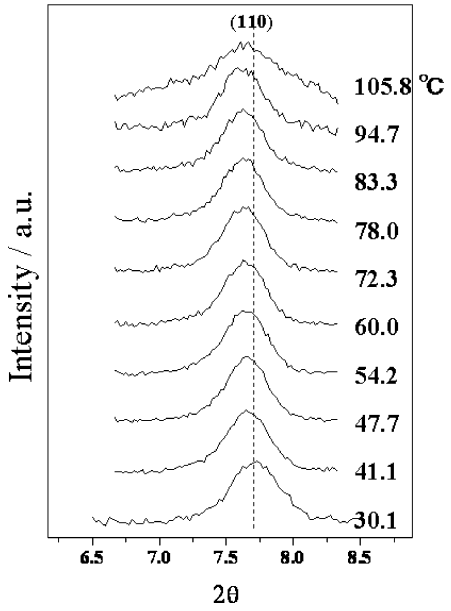

Figure 9. Temperature dependence of the X-ray diffraction of the P(HB-*co*-HHx) chloroform solution cast film sample over a temperature range from 30.1 to 105.8 °C.

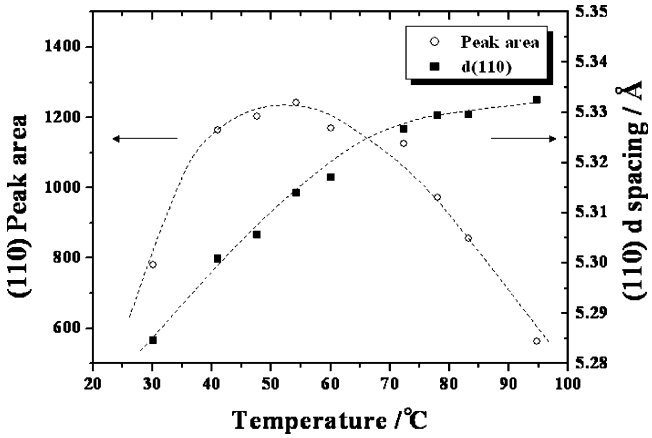

Figure 10. Temperature dependence of the peak area and *d* spacing of (110) reflection of P(HB-*co*-HHx) cast film sample from a chloroform solution.

precipitated sample changes little until about 50 °C while that of the solution cast sample increases until around 54 °C. Therefore, the maximum of the peak area around 54 °C suggests that a recrystallization of the chloroform solution cast P(HB-*co*-HHx) copolymer takes place around 54 °C.

Figure 11 shows effects of temperature on the lattice parameter *a* of the solution cast film sample. Changes in the lattice parameters of polymers can be observed under a variety of conditions.[28] Information about the changes in the lattice parameters provides insight into the forces that bind atoms and molecules in the crystal structure and the factors that determine the crystal structure. There is a slight difference in the shift of the lattice parameter *a* between the precipitated and solution cast samples (Figures 8 and 11). The change in the lattice parameter *a* of the chloroform solution cast sample is slightly larger than that of the precipitated sample. The slight difference in lattice parameter *a* comes from the difference in the crystallite size. The gradual peak shift of the WAXD pattern with temperature shows a thermal expansion of the crystalline structure of the sample. Therefore, it seems that the

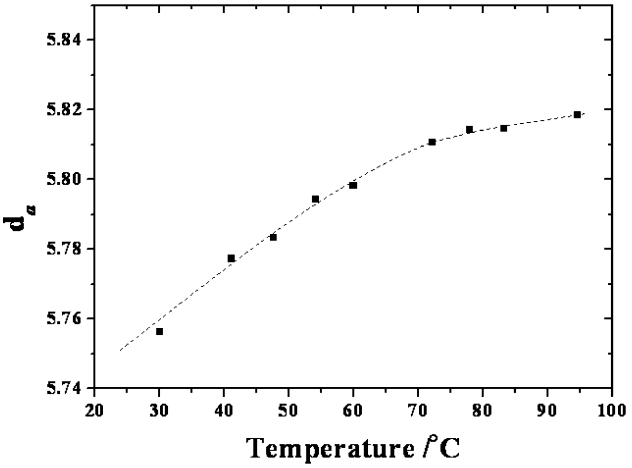

Figure 11. Temperature-dependent changes in the lattice parameter *a* of a chloroform solution cast film of P(HB-*co*-HHx).

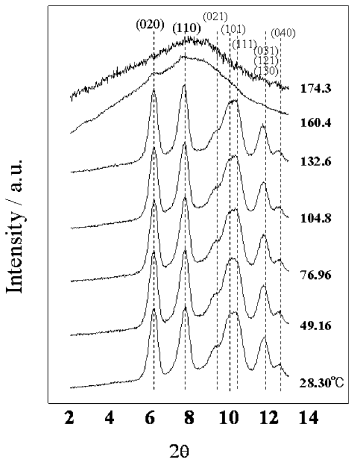

Figure 12. Temperature dependences of the X-ray diffraction of PHB homopolymer measured over a temperature range of 28.3−174.3 °C.

solution cast sample shows recrystallization process because the solution cast sample cannot assume the high-crystallinity structure and shows its own low crystallization rate.

Temperature-Dependent Variations in WAXD of PHB. Figure 12 presents a temperature dependence of the X-ray diffraction of PHB homopolymer. It shows clearly the (020), (110), (021), (101), (111), and (040) *d* spacings. Comparison of the result in Figure 12 with that in Figure 4 reveals that the crystallinity of PHB is higher than that of P(HB-*co*-HHx) precipitated sample.

Parts a and b of Figure 13 show respectively the temperature dependences of the (110) peak area and (110) *d* spacing and those of the (020) peak area and (020) *d* spacing of PHB. The melting temperature T_m of PHB was reported to be 178 °C.[22] There is a drastic drop of the (110) and (020) peak areas around 160 °C. The (110) *d* spacing of PHB shows a gradual change with temperature as in the case of the P(HB-*co*-HHx) sample, while the (020) *d* spacing shows only a small shift different from that of the P(HB-*co*-HHx) sample. The (110) peak area of P(HB-*co*-HHx) decreases from around 50 °C while that of PHB changes little at least until 140 °C, indicating that the crystallinity of PHB remains nearly unchanged until 140 °C but that of P(HB-*co*-HHx) decreases gradually from fairly low temperature (∼50 °C). The copolymerization of HHx units

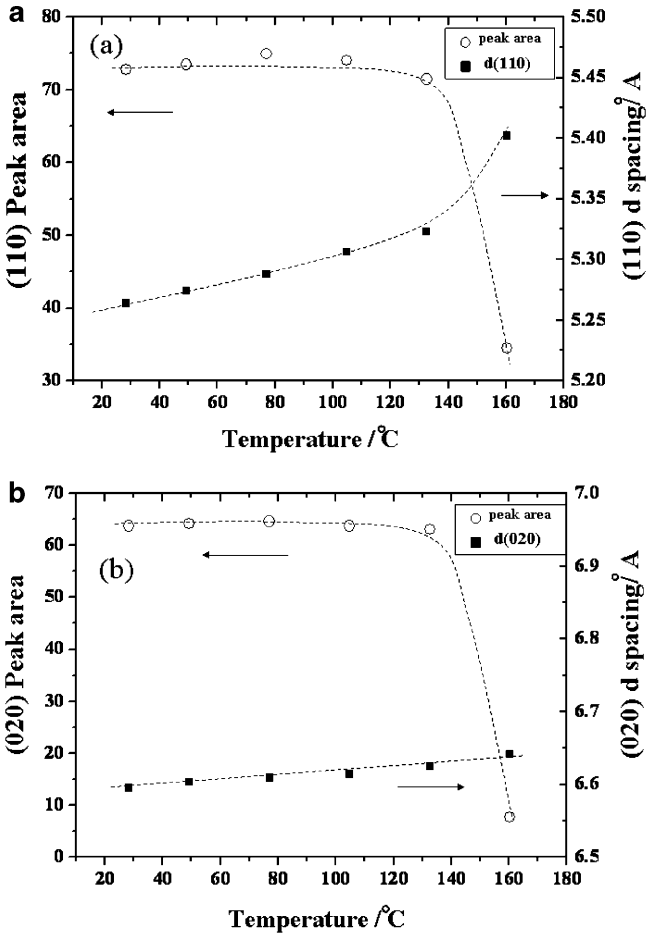

Figure 13. Temperature dependences of the peak area and *d* spacing of (a) (110) reflection and (b) (020) reflection of PHB homopolymer.

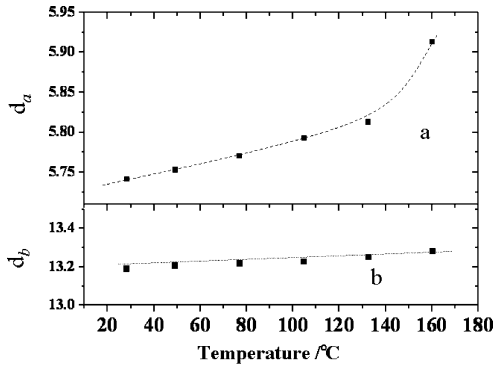

Figure 14. Changes in the lattice parameters, *a* and *b*, of the PHB homopolymer vs temperature.

in the molecular chain of PHB produces significant amounts of amorphous parts in P(HB-*co*-HHx), which change largely its thermal behavior from that of PHB.

Figure 14 shows effects of temperature on the lattice parameters of PHB. Both lattice parameters, *a* and *b*, show thermal expansion in the PHB sample. However, the thermal effects on the lattice parameters are significantly different between the lattice parameters, *a* and *b*, even in the PHB crystalline structure. P(HB-*co*-HHx) copolymer shows little expansion of the *b* axial length (Figure 8). However, PHB homopolymer shows a significant expansion of the *b* axial length, even though it is smaller than that of the *a* axial length (Figure 14), probably because the crystallinity of PHB is higher than that of P(HB-*co*-HHx) copolymer. Although our measurements were not made with high resolution, the results clearly point out the trend that the *a* axial length shows a much larger change than the *b* axial length in both P(HB-*co*-HHx) and PHB.

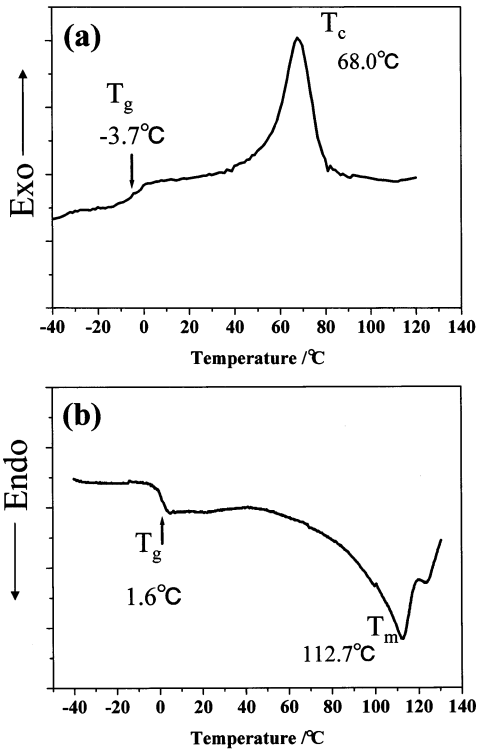

Figure 15. DSC curves of the (a) first cooling run and (b) second heating run of the precipitated P(HB-*co*-HHx) from −40 to 120 °C. Heating and cooling rates of the DSC measurements were 10 °C min^{-1}.

For both P(HB-*co*-HHx) and PHB, the lattice parameter *a* shows a significant variation by the temperature increase. This is an evidence showing that the inter- and intramolecular interactions are not so strong along the *a* axis in P(HB-*co*-HHx) and PHB crystallites. The variation of the lattice parameter *a* suggests that these interactions are those due to the C═O group and the CH_3 group, which are, in general, weak. The high crystallinity of P(HB-*co*-HHx) and PHB may be concerned with these interactions.

Thermal Analysis. Figure 15 shows the DSC curves of the (a) first cooling and (b) second heating of bulk sample of P(HB-*co*-HHx). The T_m and the glass transition temperature T_g respectively were determined from the DSC curves to be 112.7 and 1.6 °C. The appearance of intermediate states of P(HB-*co*-HV) (20.4% HV) and P(HB-*co*-HHx) (HHx = 10%) has been suggested from a small and wide endothermic premelting peak around 60 °C in the DSC measurement.[26,27] Our result of the DSC measurement of P(HB-*co*-HHx) (HHx = 12 mol %) does not show any peak around 60 °C for the bulk sample. However, variations in FT-IR spectra of a cast film of P(HB-*co*-HHx) were observed around 60 °C. To check the possible development of a peak around 60 °C in the DSC measurement, we measured DSC curves of the chloroform cast sample. The cast sample was put in a small cup for the DSC measurement. Heating and cooling rates were 20 °C min^{-1}. Figure 16 shows the DSC curves of the (a) first cooling and (b) second heating for the cast sample of P(HB-*co*-HHx). The recrystallization temperature was determined to be 51.0 °C for the cast sample in the heating process. The result of

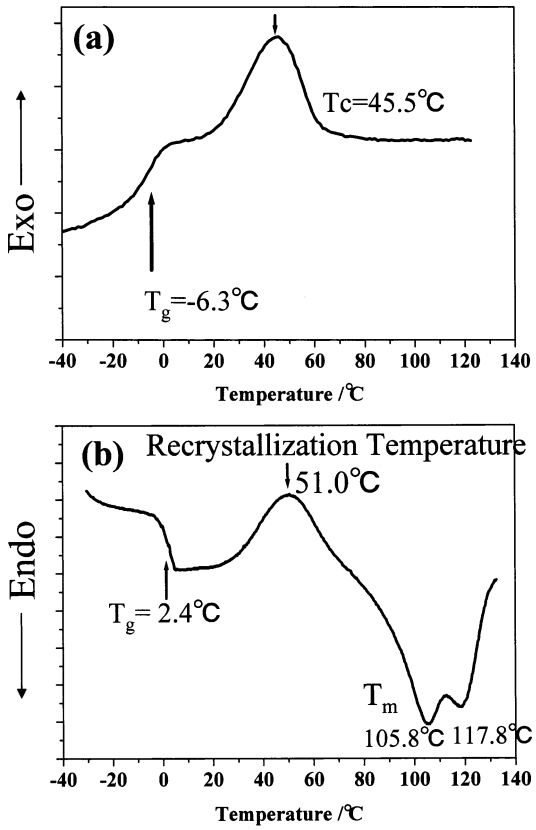

Figure 16. DSC curves of the (a) first cooling and (b) second heating run of the chloroform solution cast film sample of P(HB-*co*-HHx) from −40 to 120 °C. Heating and cooling rates were 20 °C min^{-1}.

the WAXD of the chloroform cast sample of P(HB-*co*-HHx) shows that the (110) peak area has a maximum value around 54 °C. The maximum of the (110) peak area may be ascribed to the recrystallization process of the chloroform cast sample of P(HB-*co*-HHx) (Figure 10). It is in good agreement with the DSC results of the chloroform cast sample of P(HB-*co*-HHx). Furthermore, it is noted that two peaks of T_m appear in the DSC curve of the cast sample of P(HB-*co*-HHx) (105.8 and 117.8 °C). There are two possibilities for the origin of the two peaks in the second heating cycle of DSC. One is melt and recrystallization of the sample. The other possibility is that there are two types of lamellae in the crystal.

Conclusion

The WAXD pattern of the P(HB-*co*-HHx) copolymer at room temperature shows that it has an orthorhombic system ($\alpha = \beta = \gamma = 90°$) with $a = 5.76$ Å, $b = 13.20$ Å, $c = 5.96$ Å (fiber repeat), which is identical to that of the PHB crystal system. The crystal structure and the thermal properties of precipitated and chloroform solution cast film samples of P(HB-*co*-HHx) copolymer have been investigated over the temperature range from 25 to 110 °C in the scattering angle range of $2\theta = 5-13°$. Measurements of the *d* spacing from WAXD have indicated an expansion of the (110) *d* spacing of P(HB-*co*-HHx) lattice as temperature increases. Only the *a* lattice parameter shows the thermal expansion, while the *b* lattice parameter shows very little it in the P(HB-*co*-HHx) crystallites. This suggests that there are inter- and intramolecular interactions between the C═O group and the CH_3 group because they are very closely located to each other along the *a* axis of P(HB-*co*-HHx) crystallites. The temperature-dependent variations in the (110) peak area for P(HB-*co*-HHx) and PHB have revealed that PHB keeps its high crystallinity at least until 140 °C while that of P(HB-*co*-HHx) starts decreasing from 50 °C. The copolymerization of HHx units in the molecular chain of PHB largely modifies the thermal behavior of PHB. The DSC measurements of the P(HB-*co*-HHx) between −40 and 120 °C show a recrystallization peak around 51 °C. This result is in a good agreement with the result of the WAXD of the chloroform cast sample of P(HB-*co*-HHx) that shows the maximum of the (110) peak area around 54 °C.

Acknowledgment. We thank Dr. Mike Satkowski (The Procter and Gamble Co., Cincinnati, OH) for valuable discussions. A.P. thanks the Thailand Research Fund (TRF) for financial support (Grant contact number: PHD0066/2544).

References and Notes

(1) Doi, Y. *Microbial Polyesters*; VCH Publishers: New York, 1990.
(2) Anderson, A. J.; Dawes, E. A. *Microbiol. Rev.* **1990**, *54*, 450.
(3) Lundgren, D. G.; Alper, R.; Schnaitman, C.; Marchessault, R. H. *J. Bacteriol.* **1965**, *89*, 245.
(4) Dawes, E. A. *Novel Biodegradable Microbial Polymers*; Kluwer Academic: Dordrecht, 1990.
(5) Lara, L. M.; Gjalt, W. H. *Microbiol. Mol. Biol. Rev.* **1991**, *63*, 21.
(6) Iwata, T.; Doi, Y. *Macromol. Chem. Phys.* **1999**, *200*, 2429.
(7) Barham, P. J.; Barker, P.; Organ, S. *FEMS Microbiol. Rev.* **1992**, *103*, 289.
(8) Holmes, P. A. In *Developments in Crystalline Polymers*; Bassett, D. C., Ed.; Elsevier: London, 1987; Vol. 2, p 1.
(9) Williams, S. F.; Martin, D. P. In *Biopolymers;* Doi, Y., Steinbüchel, A., Eds.; Wiley-VCH: Wienheim, 2001; Vol. 4, p 91.
(10) Marchessault, R. H.; Coulombe, S.; Morikawa, H.; Okamura, K.; Revol, J. F. *Can. J. Chem.* **1981**, *59*, 38.
(11) Barham, P. J.; Keller, A.; Otum, E. L.; Holmes, P. A. *J. Mater. Sci.* **1984**, *19*, 2781.
(12) Barham, P. J. *J. Mater. Sci.* **1984**, *19*, 3826.
(13) Satkowski, M. M.; Melik, D. H.; Autran, J.-P.; Green, P. R.; Noda, I.; Schechtman, L. A. In *Biopolymers*; Steinbüchel, A., Doi, Y., Eds.; Wiley-VCH: Wienheim, 2001; p 231.
(14) Yokouchi, M.; Chatani, Y.; Tadokoro, H.; Teranishi, K.; Tani, H. *Polymer* **1973**, *14*, 267.
(15) Cornibert, J.; Marchessault, R. H. *J. Mol. Biol.* **1972**, *71*, 735.
(16) Yoshie, N.; Menju, H.; Sato, H.; Inoue, Y. *Macromolecules* **1995**, *28*, 6516.
(17) Holmes, P. A. *Phys. Technol.* **1985**, *16*, 32.
(18) Bluhm, T. L.; Hamer, G. K.; Marchessault, R. H.; Fyfe, C. A.; Veregin, R. P. *Macromolecules* **1986**, *19*, 2871.
(19) Web site: www.nodax.com.
(20) Doi, Y.; Kitamura, S.; Abe, H. *Macromolecules* **1995**, *28*, 4822.
(21) Kobayashi, G.; Shiotani, T.; Shima, Y.; Doi, Y. In *Biodegradable Plastics and Polymers*; Doi, Y., Fukuda, K., Eds.; Elsevier: Amsterdam, 1994; p 410.
(22) Abe, H.; Doi, Y.; Aoki, H.; Akehata, T. *Macromolecules* **1998**, *31*, 1791.
(23) Kunioka, M.; Tamaki, A.; Doi, Y. *Macromolecules* **1989**, *22*, 694.
(24) Sato, H.; Murakami, R.; Padermshoke, A.; Hirose, F.; Senda, K.; Noda, I.; Ozaki, Y., to be published.
(25) Marchessault, R. H.; Morikawa, H.; Revol, F. J.; Bluhm, T. L. *Macromolecules* **1984**, *17*, 1882.
(26) Wu, Q.; Tain, G.; Sun, S.; Noda, I.; Chen, G.-Q. *J. Appl. Polym. Sci.* **2001**, *82*, 934.
(27) Tain, G.; Wu, Q.; Sun, S.; Noda, I.; Chen, G.-Q. *Appl. Spectrosc.* **2001**, *55*, 888.
(28) Davis, G. T.; Eby, R. K.; Colson, J. P. *J. Appl. Phys.* **1970**, *41*, 4316.

MA049863T